In silico analysis of *IL1RN* genetic variants in the deficiency of Interleukin-1 receptor antagonist

Joshua Pillai[1, 2*]

[1]School of Biological Sciences, University of California, San Diego, 9301 S Scholars Dr, La Jolla, 92093, CA, USA.

[2]Department of Neurosciences, University of California, San Diego, School of Medicine, 9500 Gilman Dr, La Jolla, 92093, CA, USA

*To whom correspondence should be addressed: Joshua Pillai

E-mail: jppillai@ucsd.edu

This PDF file includes:

Main Text

Figure 1-3

Table 1

Supplementary Text 1-3

Abstract

Deficiency of Interleukin-1 receptor antagonist (DIRA) is a rare autosomal recessive autoinflammatory disease caused by loss-of-function mutations in the *IL1RN* gene. Currently, limited information exists on all of its known genetic variants, particularly their impacts on the function and stability of resulting *IL1RN* mRNA and IL-1Ra proteins. To address this current gap, we analyzed 15 unique mRNA transcripts and 10 subsequent IL-1Ra. Using the biopython computational tool, we first predicted changes in molecular properties of IL-1Ra based on amino acid compositions and prior empirical models. An RNA secondary structure prediction was then conducted to identify potential local and global changes in the minimum free energy structures with RNAfold. We then performed a structural analysis of the resulting IL-1Ra and IL-1R1 complexes. After predicting the mRNA secondary structures, we report alterations in stability, base pairing, and structure. From the structural analysis of IL-1Ra, we provide insights into changes in structure (β-sheets, α-helices) and stability of the overall complex. Lastly, we evaluate the pathogenic mechanisms proposed from prior studies and discuss them in the context of this work. Overall, although further *in vivo* experimental studies are still required to investigate the mRNA structure and IL-1Ra expression, this work provides valuable preliminary insights into the pathogenic impacts of the variants on the *IL1RN* mRNA and IL-1Ra protein.

Keywords: DIRA; Mutations; IL1RN; IL-1Ra; Autoinflammatory Disease; Deficiency of Interleukin-1 Receptor Antagonist.

Highlights

- This is the first study broadly investigating the known genetic variants of DIRA disease.
- Structural analysis revealed that 80% of variants retained 3 or less β-sheets and 60% lacked any α-helices.
- All mutations appear to have a destabilizing effect on the conformation of IL-1Ra from stability data.
- Large deletion variants had an altered global mRNA structure, while nonsense and frameshift variants appear with more subtle local changes.

Abbreviations:

IL-1Ra: Interleukin-1 Receptor Antagonist

DIRA: Deficiency of Interleukin-1 Receptor Antagonist

NCBI: National Center for Biotechnology Information

PDB: Protein Data Bank

MSA: Multiple Sequence Alignment

WT: Wild Type

MFE: Minimum Free Energy

1. Introduction

Interleukin-1 receptor antagonist (IL-1Ra) is a critical member of the IL-1 family, having an important role in binding to IL-1 receptors (*1*). IL-1Ra is secreted from numerous cell types, such as immune, epithelial, and stromal cells, and is known to modulate immune and inflammatory responses (*2*). Specifically, IL-1Ra is known to competitively inhibit binding of IL-1α and IL-1β from receptors without having any detectable intracellular responses (*3*). This protein is encoded by the *IL1RN* gene, spanning approximately 400-kb on chromosome 2, with 4 isoforms variants being previously reported (*4*). Naturally, given its role in regulating inflammatory responses, IL-1Ra is important to have in balance with IL-1 as it relates to maintaining normal physiology of various tissues and organs (*5*). If imbalanced, with an overproduction of IL-1 and/or underproduction of IL-1Ra, can lead to the development of disease, as reported for gastric cancer, rheumatoid arthritis, and the deficiency of Interleukin-1 receptor antagonist (DIRA) (*5*-*6*).

DIRA is a rare autosomal recessive disease present near or at birth, and is characterized by osteomyelitis with pustulosis and systemic inflammation (*7*). With a mortality rate of 25%, there are no known patients who have reached adulthood with DIRA without prior treatment (*7*). The primary cause of this autoinflammatory disease is from loss-of-function mutations occurring in the *IL1RN* gene, leading to lower secretion of IL-1Ra. Ultimately, this results in the uncontrolled pro-inflammatory signaling of cytokines IL-1α and IL-1β, and eventually systemic inflammation in patients.

Within current literature, there have been 33 patients that have been reported up to date. Only one clinical trial (ClinicalTrials.gov ID: NCT00059748) has been reported including 9 patients from Aksentijevich et al., and the remaining in individual case reports (*8*). Due to the varying levels of reporting of patients in literature and the small population size, it is challenging to model this disease clinically (*9*). One major gap in literature is that there are no studies that have broadly investigated the known cytogenetic abnormalities and their pathogenic impacts on the resulting *IL1RN* mRNA and subsequent IL-1Ra proteins, which are critical in understanding the pathophysiology of DIRA. Ultimately, because of the clinical needs and current gap in literature for this life-threatening condition, we were motivated to thoroughly analyze all of its known genetic variants in the context of their mRNA and protein secondary structures. In order to further improve modeling of this rare disease, we sought to explore the changes in functionality and stability of these critical components.

We first began by screening prior literature and public sources to obtain the precise mRNA and protein sequences. Preliminary analysis of molecular properties were first evaluated from the protein sequences to evaluate for alterations in variants. An RNA secondary structure prediction was then performed to determine changes in stability and function of the mRNA transcripts. A structural analysis was also completed to assess for changes that resulted in poor protein expression, such as in the secondary structure and thermodynamic stability of the complex. Finally, various outcomes are discussed and directions for future studies are noted.

2. Materials and Methods

2.1. Sequence Acquisition

All cytogenetic abnormalities of known DIRA patients have been displayed in Table 1. As of June 25, 2024, there have been 33 DIRA patients and 16 genetic variations that have been reported within literature from 22 studies (*8-29*). Of all *IL1RN* genetic variants, we identified 7 unique nonsense, 3 frameshift, 4 large deletions, 1 in-frame deletion, and 1 compound mutations displayed in Table 1. We precisely obtained these counts from the recent review by Pillai et al. and a manual search on the PubMed database with the key-words on June 25, 2024: "Deficiency of Interleukin-1 Receptor Antagonist" OR "DIRA" (*30*). After review of literature, most mRNA and protein sequences were not readily available. Therefore, we were required to manually create all known variants from their associated reference mRNA sequences provided by the National Center for Biotechnology Information (NCBI). Almost all sequences (n = 15) were referred to by transcript variant 1 (NM_173842.3) with the only exception being from the variant by Abdwani et al. that used variant 2 (NM_173841.2) (*21*). Additionally, to help guide the creation of the sequences and to validate them, we used the Infevers database (http://fmf.igh.cnrs.fr/infevers/) to help catalog the nucleotide sequences of most patients (*31*). Overall, this study did not require consent or approval from an Institutional Review Board as all data was obtained from publicly available sources: NCBI, published manuscripts, and Infevers database.

Of the 16 total variants, the only one that was unable to be formulated was the large deletion variant of a 175-kb deletion on chromosome 2q involving 6 IL-1 related genes (*8, 28*). This was due to the complexity of the mutation as well as the lack of data availability and validation of the precise mRNA from the publications or Infevers database. Despite this limitation, this study was able to estimate the mRNA sequences of 15 variants, all displayed in Supplementary Material 1. We have noted whether the sequence for each variant was verified or

not by another public source, along with notes regarding discrepancies in reporting. For all experiments of this study, transcript variant 1 was used as the wild type (WT) for all comparisons unless stated otherwise.

Lastly, after obtaining the final mRNA sequences, we manually began translation of the variants in order to directly compare to the WT protein sequence. We specifically inputted the nucleotide sequence into a translation tool by Expasy (https://web.expasy.org/translate/) and confirmed the sequence with that from a bioinformatics tool (https://www.bioinformatics.org/). The protein sequences were then reviewed for completion and possible errors from the individual publications and the Infevers database. All protein sequences are provided in Supplementary Material 1.

2.2. Predicted Changes in Molecular Properties of IL-1Ra

Before performing analyses of the protein sequences, we conducted multiple sequence alignment (MSA) using Clustal Omega (version 1.2.4) from the European Molecular Biology Laboratory Bioinformatics Institute (EMBL-EBI) between the individual WT and mutant sequences to first visualize differences (*32*). We preliminarily evaluated changes in molecular properties of the resulting IL-1Ra protein for all genetic variants, such as changes in solubility or likelihood of misfolding and degrading in a test tube. In particular, we used an in-house Python script with the biopython library to measure the (i) length of amino acids, (ii) hydrophobicity, (iii) instability index, (iv) isoelectric points, (v) amino acid composition, and (vi) molecular weight of all sequences (*33*). The Python script has been made publicly available at the data repository website (https://diradisease.github.io).

2.3. RNA Secondary Structure Prediction

Before evaluating the 3D structures of the IL-1Ra proteins, we wanted to elucidate the pathogenic effects of all mutations on the *IL1RN* mRNA transcripts as little information currently exists on it. Mendonca et al. previously hypothesized that a truncated and unstable mRNA transcript, in addition to the mutation, may lead to little or no expression of IL-1Ra, eventually causing DIRA, but this predicted mechanism has yet to be investigated (*9*). Therefore, we conducted a secondary structure prediction to investigate the stability and function of the transcripts (*34*). Using RNAfold from ViennaRNA Package 2 (*35*), we inputted the mutant and WT sequences into the software and obtained the RNA structures. Specifically, we collected all thermodynamic values of the predicted structure from RNAfold to better understand the context of stability, displayed in Supplementary Material 2. It must be noted that for Abdwani et al., the structure was compared to a different WT (transcript variant 2) than all other variants, and defined as 'WT (version 2)' in the results (*21*).

A supplemental analysis was also evaluated for changes in base-pairing probabilities and local/global secondary structure. We used an in-house Python script to overlay base-pairing probabilities of the WT and mutant RNAs (*35*) for comparison of secondary structural changes. The resulting secondary structures were also visually compared. Lastly, we exported the mountain plots of all predicted structures to examine changes within individual positions. Overall, the purpose of these additional analyses were to further evaluate other aspects of stability and function that may not be reflected by the thermodynamic metrics alone.

2.4. Modeling the Protein Complex

Following RNA structure predictions, we took all protein sequences (n = 16) and performed a structural analysis to evaluate changes in (i) secondary structure and (ii) stability in the complex between IL-1Ra and IL-1R1. Due to a lack of newer and lower resolution experimental models provided from the Protein Data Bank (PDB), we initially considered using AlphaFold 2 (version 1.5.5), a state-of-the-art machine learning model for predicting protein structure by Google DeepMind (*36*), to retrieve their predicted 3D structures with ColabFold (*37*). However, after preliminary testing with AlphaFold, we found that the models provided an incorrect secondary structure, predicting 13 β-strands instead of the confirmed 12 strands, and therefore returned to the experimental model.

We specifically followed the experimental model (1IRA) reported by Schreuder et al. that was obtained through X-Ray crystallography (*38*). It must be noted that the partial sequence at the *N*-terminal segment is not included in the 3D structure (positions 1-31), and we modified our sequence to adjust for this difference. Using the open-source PyMOL software, we uploaded the 3D structure of the experimental model, labeling the α-helices and β-strands of IL-1Ra. After modeling all protein complexes, structural files (.mdb), PyMOL files (.pse), and images (.png) were loaded onto the data repository website (https://diradisease.github.io).

One limitation with modeling some of the variants was that PyMOL does not currently have capability to model complex mutations. For Jesus et al., the software was unable to predict new bonding between two partial sequences caused from an in-frame deletion. With Sözeri et al., although similar to other nonsense mutations like Aksentijevich et al. (N52KfsX25) in type and

context, the resulting amino acid sequence became too long to reliably predict new structures and interactions after the point of mutation. With the cases of Kuemmerle-Deschner et al. and Ulusoy et al., although PyMOL is able to predict these nonsense mutations, the sequences were too short to be used in altering the experimental model as the *N*-terminal amino acids are not present. This can also be explained in context for the sequence from Mendonca et al. of the large deletion variant.

Lastly, an exception to our methodology for predicting the 3D protein structure of the variants was with Abdwani et al. that was able to be predicted because of its similarity in sequence to the experimental structure (*21*). From alternative splicing, we found that the resulting protein sequence was similar except for the *N*-terminal amino acids that were already missing from the experimental model, and therefore could be predicted. Overall, we were able to model 10 of the 15 variants and have them directly compared to the WT.

2.5. Protein Structural Analysis

For structural analyses of the resulting proteins, we noted important features of the WT IL-1Ra before comparing structures of the genetic variants. The known structure of the WT is composed of 12 β-strands and 3-10 α-helices (*39*). β1, β4, β5, β8, β9 and β12 are particularly important for the formation of the protein as they are critical to forming its six-stranded β-barrel (*40*). In the PDB, the experimental model by Schreuder et al. reported 4 α-helices (*38*). Herein, we sought to observe changes in (i) stability in interactions between IL-1Ra and IL-1R1 from the WT and (ii) structural changes that led to misfolding of the β-barrel. In Supplementary Material 3, the positions of β-strands and α-helices were explicitly noted from the experimental model, along

with those of the mutant sequences, to effectively measure changes in secondary structure of proteins. We also predicted changes in stability of the resulting complexes from the solvation free energy of folding (ΔG) by PDBePISA offered from the PDB (*41*). This was a critical metric to validate for direct comparison of the predicted stability measured empirically assuming *in vitro* conditions from the instability indexes. Additionally, it would be a valuable finding to evaluate the overall expression of IL-1Ra, particularly with regards to misfolding and degradation.

3. Results

3.1. Molecular Properties of IL-1Ra Variants

All preliminary analyses of changes in molecular properties of the IL-1Ra protein for each genetic variant is shown in Figure 1. We have displayed the amino acid lengths in Panel B, hydrophobicity in Panel C, isoelectric points in Panel D, instability indexes in Panel E, amino acid distribution in Panel F, and molecular weights in Panel G. Of the protein sequences, most variants resulted in a shorter amino acid sequence compared to the WT with exception to the c.396delC substitution by Sözeri et al. that resulted in a frameshift mutation (*12*). From a significant loss of amino acids in 14 variants (~ 93.3%), it would be expected that the resulting protein would be missing significant secondary structures and have a lower molecular mass. With consideration to polarity, 11 variants (~ 73.3%) remained hydrophilic similar to the WT. From the variants that became hydrophobic ($n = 4$), the most drastic change was by Ulusoy et al. (c.76C>T) and Kuemmerle-Deschner et al. (c.62C>G) because there was an increase in the distribution of leucine that made the sequences more hydrophobic from the WT (*11, 16*). With consideration to changes in isoelectric points (pl), 14 variants (~ 93.3%) had a higher pH of no

net charge than the WT. The isoelectric points of the proteins likely increased because there was a higher distribution of more basic amino acids, particularly arginine and lysine.

Lastly, the most important property to assess the IL-1Ra proteins were their instability indexes. From all proteins including the WT, 15 proteins (93.7%) were considered unstable. Of the unstable proteins, 13 variants (86.6%) were calculated to be more stable than the WT. Only 1 variant had a predicted structure that was considered stable from the large deletion variant by Mendonça et al., having a score below 40 (*9*). Overall, these predicted results were unexpected as truncated and altered sequences in critical domains are typically expected to make proteins more unstable. However, it must be noted that the biopython library uses an empirical model that predicts instability based on amino acid composition and dipeptide sequences, and may not consider other complex cellular interactions assuming *in vitro* conditions. Therefore, we also performed further stability analyses *in silico* during structural analysis of the IL-1Ra variants for validation of these findings.

3.2. Stability of mRNA Transcripts of Variants

From RNA secondary structure predictions, we first stored optimal structure at the minimum free energy (MFE) values and the thermodynamic ensemble to evaluate the stability of all transcripts. We have displayed the general trends of these thermodynamic metrics among the optimal structures of variants in Figure 2 (Panel A and B) and Supplementary Material 2. For MFE, we found that 11 variants (73.3%) maintained a similar stability to the WT at approximately -545 kcal/mol, along with Abdwani et al. at -606 kcal/mol to its WT (*21*). Interestingly, the three variants that had a lower stability than all other structures were the 3 large deletion mutations

reported by Mendonça et al. (22,216 bp deletion) and Urbaneja et al. (c.116+774del2253 and c.318+2T>G) by 9.3-11.4% from the WT (*9, 22*). A similar trend was also observed for ensemble free energies of all variants, with a decrease in stability by 8.6-11.1% for these 3 mutants from the WT. From both thermodynamic metrics, it can also be observed that all other nonsense, frameshift, and deletion variants were within 10 kcal/mol of the WT value. Overall, from these broad trends, it can be suggested that substitution and deletion mutations appeared to have a much smaller impact than those of large deletion in the RNA thermodynamic stability. This is expected as these large deletion variants resulting in mRNAs have a truncated transcript and appear to have the most missing coding sequences resulting from deletions of critical exons. We have also investigated these results and other predicted trends further in evaluation of the RNA secondary structures and altered base-pairing probabilities.

Our data repository website (https://diradisease.github.io) has displayed all predicted secondary structures of the WT with comparison to each variant. The website has also provided interactive dot plots for comparing the base-pairing probabilities of the different variants from the in-house Python script. For a uniform comparison of all variants, we have displayed mountain plots of the MFE and ensemble structures represented by height vs. position curves, where helices are represented by the slopes, hairpin loops by peaks, and loops by plateaus on the plots. The graphs also include a measure of entropy, where higher values represent points of greater instability in RNA structure. After analysis of mountain plots, we found that major alterations occurred in the secondary structure of all 3 large deletion variants, where there appears to be missing helices, hairpins, and loops of the WT. Of the MFE structures, we observed that all other mutations appeared to have a similar secondary structure except for

localized changes in 3 nonsense and all frameshift variants, particularly with helices and hairpins as the MFE does not appear to have any plateaus. All mountain plots of variants are available in Supplementary Material 2 for further comprehensive analysis.

From all predicted structures, we observed not only drastic changes in base-pairing probabilities but also disruptions in global structure for all large deletion variants ($n = 3$). For the nonsense variants, the structural impacts and disruptions varied for different mutations, but it is clear that small changes in local structure or their pairing occurred. One exemplar nonsense variant is from Altiok et al. (c.355C>T) that retained almost a completely similar structure except for changes in base-pairing for one hairpin site (*14*). Another instance is with Aksentijevich et al. (c.160C>T) that had retained a similar global structure but was predicted to have a missing hairpin loop and changes in pairing of another from the WT (*8*). Within both of these exemplar variants, there appeared to be very small changes in probabilities, but the extent of disruptions differ from each individual variant. For comparison to the results of nonsense variants, we observed variations in frameshift, and found that the extent of changes varied similarly to those of the substitution mutants. Overall, our preliminary analyses of all mutants suggest that the variants with substitution and point deletions had significant disruptions in base-pairing probabilities and local structures (missing hairpins, helices, etc) that likely impacted their function, but still allowed them to retain a similar global structure, and therefore yielding a close thermodynamic stability to the WT. All individual comparisons between the variant and the WT structures are available from the data repository website for further comprehensive analysis.

3.3. Structural Changes of IL-1Ra and IL-1R1 Complexes

The ligand-receptor complexes predicted by the experimental model have been displayed for the 10 variants in Figure 3 (Panel A to Panel J). Our structural analysis included 6 nonsense variants, 1 frameshift, 1 compound, and 2 large deletion variants. The changes in secondary structures of the proteins have been visualized in Figure 2 (Panel C and D). For all predicted complexes, we have labeled the β-sheets in yellow, α-helices in magenta, IL-1R1 in blue, and all other structural components of IL-1Ra in orange. Of all proteins, 60% lacked any α-helices and only 20% retained more than half of the WT. The most critical aspect of the secondary structure was with changes in β-sheets, where 80% of variants had 3 β-sheets (β1, β2, β3) or less. The only two exceptions were by Abdwani et al. (Gln122Ter) and Altiok et al. (Q199X) that retained up to 7 β-sheets (*14, 21*). When considering the WT structure of IL-1Ra, where β1, β4, β5, β8, β9, and β12 are essential to forming a six-stranded antiparallel β-barrel, the variants only retained 50% or less of the necessary components. From the lack of critical components in secondary structure, we can pose that IL-1Ra did not properly fold for all mutants and therefore likely lead the proteins to be non-functional.

For changes with amino acid bindings between the two proteins, we calculated the predicted protein stabilities *in silico*. From PDBePISA, we obtained the ΔG for all variants and later manually calculated ΔΔG. The results of ΔG have been visualized in Figure 3 (Panel D). We found that IL-1Ra naturally has a lower stability (-135.8 kcal/mol) than IL-1R1 (-282 kcal/mol), and that all mutations appear to have a destabilizing effect on the conformation of the resulting proteins. All values of ΔΔG were positive among variants, displayed in Supplementary Material 3 and Panel D, suggesting that the proteins are less stable and have a lower thermodynamic favorability than those of the WT. The ΔG of the variants also suggests that there

is a lower binding affinity of IL-1Ra to IL-1R1, potentially disrupting known interactions, and creating an unstable complex.

The predicted trends of ΔG are also supported by the structural changes observed in the type of alteration across variants. The data strongly supports that the magnitude of disruptions in secondary structure and misfolding can particularly impact the stability, and possibly can relate to the severity of DIRA. For instance, the structures of variants of Abdwani et al. (Gln122Ter) and Altiok et al. (Q199X) had the smallest decrease in stability compared to all other mutants because they retained the most α-helices and β-strands, and therefore was least prone to misfolding and destabilization (*14, 21*). Conversely, variants that resulted in the least stable structure, specifically those reported by Aksentijevich et al. (Q54X), Stenerson et al. (E77X/T47Tfs*4), Mendonça et al. (Q45X), and Urbaneja et al. (p.Ile40Glnfs*6), had 2 or less β-strands (*8, 18, 19, 22*). Urbaneja et al. previously stated that their reported variants were likely a lethal form of DIRA due to the alteration in the WT (*22*), which strongly suggests a correlation between the extent of instability and structural loss with the severity of DIRA. However, further evidence is required to confirm this potential correlation.

4. Discussion

To the best of our knowledge, this is the first study to conduct a broad analysis of known *IL1RN* genetic variants for DIRA disease. This short communication focused on elucidating the structural and functional impact of all variants on the mRNA transcripts, and those of the resulting IL-1Ra in its role of antagonizing signaling of IL-1R1.

Within the RNA secondary structure predictions, we first calculated the MFE and ensemble free energy structures of all 15 variants and compared them to their associated WT. We then conducted follow-up analyses by examining secondary structures, base-pairing probabilities, and mountain plots provided by RNAfold. From our predictions, we found that the mRNA structure of large deletion variants caused global changes in secondary structure, making them more unstable than the WT transcript. We also observed that the other variants, particularly the nonsense and frameshift variants, appeared to have much minute changes in local structures while retaining a similar global structure overall. This rendered their transcripts to be similar in stability to the RNA structure of the WT. However, even though thermodynamically stable, the mutations still impacted critical coding sequences that could potentially alter their function, warranting the need of this study to evaluate the resulting proteins for their stability and protein folding.

From our structural analysis of the IL-1Ra and IL-1R1 complexes, the experimental model was able to predict the 3D features of 6 nonsense variants (85.7%), 1 frameshift (33.3%), 1 compound, and 2 large deletion variants (33.3%). Of the structural components of the WT, a majority (60%) of mutants were missing all α-helices and most (80%) retaining only 25% or less (β1, β2, β3) of the necessary β-sheets. Within IL-1Ra, the antiparallel β-barrel is the most essential component in the WT, and the model predicted that all variants retained 50% or less of the necessary β-sheets. We then evaluated the stability of the resulting proteins *in silico* (ΔG and ΔΔG), and found that all mutations had a destabilizing effect on the conformation of IL-1Ra. From the data, it was also suggested that the extent of structural loss and instability could potentially relate to the severity of the disease. For instance, large deletion variants such as those

modeled for Urbaneja et al. were missing almost all structures and were among the least stable proteins, and were suggested by the original report to be a lethal form of DIRA.

This study also supports the original hypothesis of Mendonca et al. that a short and unstable mRNA transcript, along with the mutations, may result in poor expression of IL-1Ra in the context of large deletion mutations (*9*). From the RNA secondary structure prediction, we found that the large deletion variant reported by Mendonca et al. had a much lower stability among all other variants and resulted in major changes in its global structures, potentially altering its function. This trend was also observed with other large deletion variants (i.e. Urbaneja et al.) evaluated in this study, and can possibly be explained by the *in vivo* results presented by these studies.

From quantitative polymerase-chain-reaction assays, relative *IL1RN* mRNA expression was greatly diminished in the two variants by Urbaneja et al. and completely absent from the one by Aksentjevich et al. (175-kb deletion, not investigated in this study) (*8, 22*). Furthermore, the variant from Mendonca et al. had the deletion spanning the promoter, likely heavily impacting transcription, and diminishing the resulting mRNA expression (*9*). It may be possible that the large deletions could be hindering transcriptional regulation or the changes in the mRNA stability and secondary structure causes them to be more prone to degradation, and therefore yielding lower expression. We recommend future studies explore these molecular mechanisms not only for these variants, but also other nonsense and frameshift variants for comparison, beyond the preliminary *in silico* prediction data on stability and structure provided from this

study. The hypothesis by Mendonca et al. appears to be true in context of the large deletion variants but further evaluation is required for the other variant types.

Lastly, our results of this short communication may also be informative to studies evaluating the efficacy of anakinra, a recombinant human IL-1Ra, that is the primary treatment approved by the U.S. Food and Drug Administration on December 22, 2020 (*42*). Side effects of anakinra have been previously reported in DIRA patients as elevated acute-phase reactants, urticarial rashes, and respiratory distress and death (*30*). Specifically, Aksentijevich et al. (c.160C>T), Mendonca et al., Kuemmerle‐Deschner et al., and Ziaee et al. reported patients that experienced these side effects (*8, 9, 11, 20*). Mendonca et al. previously suggested that the allergic reaction in patients after receiving anakinra is likely a humoral immune response that developed after receiving a protein that was originally deficient (*9*). Their study hypothesized that truncations or complete absence of IL-1Ra may be associated with the risk of developing an immune response to anakinra (*9*). Interestingly, the variants were majority nonsense (75%) and the outlier was a large deletion variant. Due to the low sample of patients with side effects (n = 4), broad hypotheses between the extent of impact from the mutation and the risk of developing an immune response may not be possible without further *in vivo* experimental protocols in future studies.

Lastly, there are two limitations of this study that must be noted: (1) RNA prediction data and (2) mRNA and protein sequences. Within this short communication, we focused on predicting the RNA secondary structure using the MFE folding method given its high accuracy and popularity when RNA homologous information is limited (*43*). We recommend future

studies evaluate various approaches other than MFE for the prediction as well as also incorporating experimental techniques (i.e. NMR, X-Ray Crystallography, cryo-EM) to evaluate its structures. The data collected from this study are solely provided for preliminary prediction data on the *IL1RN* mRNA transcripts. Secondly, because of the poor reporting of variants in literature, this study was required to formulate the precise sequences and validate them with the results of the individual publications. While most sequences were able to be validated either through the published manuscripts or the Infevers database, the mRNA and protein sequences of Mendonca et al. and Urbaneja et al. (c.116+774del2593) were not validated to the same extent as other sequences and the discrepancies are described in the Supplementary Material. Furthermore, as of July 12, 2024, the mutation described in Ziaee et al. and those reported for it in the Infevers database has discrepancies, where the Infevers report was used in this study. Overall, this study focused on the alterations on the WT stability and function from individual mutations and does not account for any other biological phenomena.

Despite the mRNA structure prediction data being *in silico* and the need for future studies to evaluate its structure *in vivo*, the data presented from the structural analysis are accurate for the 10 variants presented. The methodology used for the structural analyses of this study was similarly used by the variant from Altiok et al. previously, and this study was able to replicate the same findings (structural data) presented by the study. Additionally, Jesus et al. partially conducted the same methodology for the in-frame deletion variant, but did not directly generate the structure because of the same limitations described in this study. However, the predicted structural changes reported by the variant by Jesus et al. were able to be replicated by this study. Both of these studies also did not measure for changes in thermodynamic stability of the protein

complexes. To the best of our knowledge, no other variants have been modeled using this methodology for structural analysis of the IL-1Ra and IL-1R1 complexes evaluated in this study.

5. Conclusion

DIRA is an ultra-rare autosomal recessive autoinflammatory disease caused by loss-of-function mutations in the *IL1RN* gene. Currently, no studies have broadly investigated the genetic variants of this life-threatening disease, and particularly their pathogenic impacts on the resulting mRNA and protein secondary structures. Herein, we first evaluated for changes in the molecular properties of IL-1Ra proteins. We then conducted a secondary structure prediction of 15 *IL1RN* mRNA transcripts, where changes in components and base-pairing were noted from local and global MFE structures. Finally, a structural analysis was performed, where changes in secondary structure and stability were evaluated. Overall, this study may be informative to future studies attempting to clinically model DIRA as well as for drug evaluations of its primary treatment, anakinra.

Figure Description.

Figure 1. The experimental model of the IL-1Ra and IL-1R1 complex is displayed in Panel A. The number of amino acids in each protein sequence is shown in Panel B, where most variants resulted in major truncations in size except c.396delC. Panel C displays the changes in hydrophobicity of sequences, with most remaining similar to the WT. Panel D shows the isoelectric points, with most mutations having a higher pH to be completely neutral compared to the WTs. Most proteins retained a lower instability to the WT plotted in Panel F when considered *in vitro*. The distribution of amino acids for all sequences is displayed in Panel E. Lastly, Panel G shows the molecular weight of all variants based on amino acids.

Figure 2. The MFE structure of all variants is shown in Panel A, where most variants retained a similar value to their associated WT, with the exceptions being of large deletion variants that were much less stable. Panel B displays the weighted average of thermodynamic free ensemble energy that serves as a confirmation for Panel A. The number of β-sheets and α-helices for the variants is displayed in Panel C. Finally, Panel D displays ΔG values that determine the stability of the molecular interaction of the complexes between IL-1Ra and IL-1R1, and ΔΔG shows how the conformation of the WT complex changes after the resulting mutations.

Figure 3. The ribbon diagram of 10 IL-1Ra and IL-1R1 complexes are displayed. β-sheets are labeled in yellow, α-helices in magenta, IL-1R1 in blue, and all other structural components of IL-1Ra in orange. The 'x' markers are water molecules that were kept from the original experimental model for imaging, but were removed during structural analysis.

Supplementary Information.

Supplementary Material 1. The mRNA and protein sequences have been provided for the genetic variants along with their associated WT. We have also provided all comments on discrepancies and limitations for individual sequences unless stated otherwise.

Supplementary Material 2. The predicted thermodynamic data for all individual mRNA transcripts have been provided along with their citation to the RNAfold website. Mountain plots have also been provided along with comments on changes in structure of the 15 variants. Lastly, the dot plots of base-pairing probabilities along with images of the secondary structures are provided with directions to the data repository website.

Supplementary Material 3. The amino acids forming individual α-helices and β-strands have been noted and highlighted for reference to the 10 variants. We have also provided highlights to the secondary structure elements that were retained by the variants as well as new structures that are formed that were not observed in the original WT.

Acknowledgements: The study received no funding. **Author Contributions:** J.P. conducted all background research, created experimental designs, performed experiments, conducted the data analysis, and wrote the manuscript. **Competing Interest Statement:** The author declares no financial or non-financial competing interests. **Data Availability:** The data used in this study was retrieved from publicly available sources. All supporting data and analysis is available in Supplementary Materials 1-3 and data repository website (https://diradisease.github.io). Any further inquiries can be sent to the corresponding author.

References.

1. Arend, W. P., Malyak, M., Guthridge, C. J. & Gabay, C. INTERLEUKIN-1 RECEPTOR ANTAGONIST: Role in Biology. *Annual Review of Immunology* **16**, 27–55 (1998).
2. Perrier, S., Darakhshan, F. & Hajduch, E. IL‑1 receptor antagonist in metabolic diseases: Dr Jekyll or Mr Hyde? *FEBS Letters* **580**, 6289–6294 (2006).
3. Arend, W. P. Interleukin-1 receptor antagonist. in *Advances in immunology* 167–227 (1993). doi:10.1016/s0065-2776(08)60535-0.
4. Carrol, E. D. *et al.* The IL1RN Promoter rs4251961 Correlates with IL-1 Receptor Antagonist Concentrations in Human Infection and Is Differentially Regulated by GATA-1. *The Journal of Immunology* **186**, 2329–2335 (2011).
5. Arend, W. P. The balance between IL-1 and IL-1Ra in disease. *Cytokine & Growth Factor Reviews* **13**, 323–340 (2002).
6. Fang, Z., Jiang, J. & Zheng, X. Interleukin-1 receptor antagonist: An alternative therapy for cancer treatment. *Life Sciences* **335**, 122276 (2023).
7. Diaz, A. Deficiency of the interleukin-1 receptor antagonist (DIRA). in *Springer eBooks* 69–83 (2019). doi:10.1007/978-3-319-96929-9_6.
8. Aksentijevich, I. *et al.* An Autoinflammatory Disease with Deficiency of the Interleukin-1–Receptor Antagonist. *New England Journal of Medicine* **360**, 2426–2437 (2009).
9. Mendonça, L. O. *et al.* Deficiency of interleukin-1 receptor Antagonist (DIRA): report of the first Indian patient and a novel deletion affecting IL1RN. *Journal of Clinical Immunology* **37**, 445–451 (2017).

10. Thangaraj, A. *et al.* All lytic bone lesions are not osteomyelitis- Think of DIRA! *Rheumatology* (2024) doi:10.1093/rheumatology/keae298.

11. Kuemmerle‐Deschner, J. *et al.* New variant in the IL1RN-gene (DIRA) associated with late-onset, CRMO-like presentation. *Rheumatology* **59**, 3259–3263 (2020).

12. Sözeri, B., Gerçeker-Türk, B., Yıldız-Atıkan, B., Mir, S. & Berdeli, A. A novel mutation of interleukin-1 receptor antagonist (il1rn) in a dira patient from turkey: diagnosis and treatment. *The Turkish Journal of Pediatrics* **60**, 588–592 (2018).

13. Jesus, A. A. *et al.* A novel mutation of IL1RN in the deficiency of interleukin-1 receptor antagonist syndrome: Description of two unrelated cases from Brazil. *Arthritis and Rheumatism* **63**, 4007–4017 (2011).

14. Altiok, E. *et al.* A novel mutation in the interleukin-1 receptor antagonist associated with intrauterine disease onset. *Clinical Immunology* **145**, 77–81 (2012).

15. Sakran, W. *et al.* Chronic recurrent multifocal osteomyelitis and deficiency of interleukin-1–receptor antagonist. *The Pediatric Infectious Disease Journal* **32**, 94 (2013).

16. Ulusoy, E. *et al.* Interleukin-1 receptor antagonist deficiency with a novel mutation; late onset and successful treatment with canakinumab: a case report. *Journal of Medical Case Reports* **9**, (2015).

17. Kutukculer, N. *et al.* Deficiency of Interleukin-1 Receptor Antagonist: A Case with Late Onset Severe Inflammatory Arthritis, Nail Psoriasis with Onychomycosis and Well Responsive to Adalimumab Therapy. *Case Reports in Immunology* **2019**, 1–6 (2019).

18. Stenerson, M. *et al.* The first reported case of compound heterozygous IL1RN

mutations causing deficiency of the interleukin-1 receptor antagonist. *Arthritis and Rheumatism* **63**, 4018–4022 (2011).

19. Mendonça, L. O. *et al.* A case report of a novel compound heterozygous mutation in a Brazilian patient with deficiency of Interleukin-1 receptor antagonist (DIRA). *Pediatric Rheumatology Online Journal* **18**, (2020).

20. Ziaee, V. *et al.* Homozygous IL1RN Mutation in Siblings with Deficiency of Interleukin-1 Receptor Antagonist (DIRA). *Journal of Clinical Immunology* **40**, 637–642 (2020).

21. Abdwani, R., Abdalla, E., Masilhi, B. A., Shalaby, A. & Al‐Maawali, A. Novel mutation in interleukin 1 receptor antagonist associated with chronic diarrhoea in infancy. *Journal of Paediatrics and Child Health* **58**, 186–188 (2021).

22. Urbaneja, E. *et al.* Case report: Novel compound heterozygous IL1RN mutations as the likely cause of a lethal form of deficiency of interleukin-1 receptor antagonist. *Frontiers in Immunology* **15**, (2024).

23. Schnellbacher, C. *et al.* Deficiency of interleukin‐1 receptor antagonist responsive to anakinra. *Pediatric Dermatology* **30**, 758–760 (2012).

24. Rivera-Sepulveda, A., Colón-Fontánez, F., López, M. & Puig-Ramos, G. Deficiency of interleukin-1 receptor Antagonist: new genetic autoinflammatory disease as a diagnostic challenge for pediatricians. *Journal of Pediatric Genetics* **12**, 227–232 (2021).

25. Suri, D. *et al.* Spectrum of Systemic Auto-Inflammatory Diseases in India: A Multi-Centric Experience. *Frontiers in Immunology* **12**, (2021).

26. Thacker, P. G., Binkovitz, L. A. & Thomas, K. B. Deficiency of interleukin-1-receptor

antagonist syndrome: a rare auto-inflammatory condition that mimics multiple classic radiographic findings. *Pediatric Radiology* **42**, 495–498 (2011).

27. Brau-Javier, C. N., Gonzales-Chavez, J. & Toro, J. R. Chronic cutaneous pustulosis due to a 175-kb deletion on chromosome 2q13. *Archives of Dermatology* **148**, 301 (2012).

28. Reddy, S. *et al.* An autoinflammatory disease due to homozygous deletion of theIL1RNLocus. *New England Journal of Medicine* **360**, 2438–2444 (2009).

29. Minkis, K. *et al.* Interleukin 1 receptor antagonist deficiency presenting as infantile pustulosis mimicking infantile pustular psoriasis. *Archives of Dermatology* **148**, (2012).

30. Pillai, K., Pillai, J. & Ling, J. Analysis of Anakinra Therapy for the Deficiency of Interleukin-1 Receptor Antagonist through Clinical Evidence. *Journal of Clinical Medicine* **13**, 1026 (2024).

31. Touitou, I. *et al.* Infevers: An evolving mutation database for auto-inflammatory syndromes. *Human Mutation* **24**, 194–198 (2004).

32. Madeira, F. *et al.* The EMBL-EBI Job Dispatcher sequence analysis tools framework in 2024. *Nucleic Acids Research* (2024) doi:10.1093/nar/gkae241.

33. Cock, P. J. A. *et al.* Biopython: freely available Python tools for computational molecular biology and bioinformatics. *Bioinformatics* **25**, 1422–1423 (2009).

34. Roy, B. & Jacobson, A. The intimate relationships of mRNA decay and translation. *Trends in Genetics* **29**, 691–699 (2013).

35. Gruber, A. R., Lorenz, R., Bernhart, S. H., Neubock, R. & Hofacker, I. L. The Vienna RNA Websuite. *Nucleic Acids Research* **36**, W70–W74 (2008).

36. Jumper, J. *et al.* Highly accurate protein structure prediction with AlphaFold. *Nature* **596**, 583–589 (2021).

37. Mirdita, M. *et al.* ColabFold: making protein folding accessible to all. *Nature Methods* **19**, 679–682 (2022).

38. Schreuder, H. *et al.* A new cytokine-receptor binding mode revealed by the crystal structure of the IL-1 receptor with an antagonist. *Nature* **386**, 194–200 (1997).

39. Fields, J. K., Günther, S. & Sundberg, E. J. Structural basis of IL-1 family cytokine signaling. *Frontiers in Immunology* **10**, (2019).

40. Veerapandian, B. Structure and function of interleukin-1, based on crystallographic and modeling studies. *Biophysical Journal* **62**, 112–115 (1992).

41. Krissinel, E. & Henrick, K. Inference of Macromolecular Assemblies from Crystalline State. *Journal of Molecular Biology* **372**, 774–797 (2007).

42. Sobi. FDA Approves KINERET® (anakinra) for the Treatment of Deficiency of IL-1 Receptor Antagonist (DIRA). *Sobi* (2023).

43. Zhao, Y., Wang, J., Zeng, C. & Xiao, Y. Evaluation of RNA secondary structure prediction for both base-pairing and topology. *Biophysics Reports* **4**, 123–132 (2018).

Table 1. Cytogenetic abnormalities reported in DIRA patients (*n* = 33).

Cytogenetic Abnormalities	Sample Size	Mutation	Reference
22,216 bp deletion	2	Large Deletion	Mendonca et al. Thangaraj et al.
c.62C>G; p. Ser21*	1	Nonsense	Kuemmerle-Deschner et al.
c.396delC, stop codon c534 position	1	Frameshift	Sözeri et al.
c.213_227delAGATGTGGTACCCAT; p.Asp72_Ile76del	2	In-frame Deletion	Jesus et al.
c.229G>T; p.Gly77	5	Nonsense	Aksentijevich et al.
c.355C>T; p.Gln119*	2	Nonsense	Altiok et al.
c.160C>T; p.Gln54*	3	Nonsense	Aksentijevich et al. Sakran et al.
c.156_157del; p.Asn52Lysfs*25	1	Frameshift	Aksentijevich et al.
c.76C>T; p.Arg26*	2	Nonsense	Ulusoy et al. Kutukculer et al.
c.229G>T; p.Gly77* and c.140delC; p.T47TfsX4	1	Compound Nonsense and Frameshift	Stenerson et al.
c.133C>T; p.Gln45*	1	Nonsense	Mendonça et al.
c.156del; p.Asn52Lysfs*4	1	Frameshift	Ziaee et al.
c.364C>T;p.Gln122Ter	1	Nonsense	Abdwani et al.
c.318+2T>G; p.Glu69Glyfs*2	1	Large Deletion	Urbaneja et al.
c.116+774del2593; p.Ile40Glnfs*6	1	Large Deletion	Urbaneja et al.
c.−64_1696del; p.IL1F9_IL1RNdel*	6	Large Deletion	Aksentijevich et al. Brau-Javier et al. Reddy et al. Minkis et al. Schnellbacher et al. Rivera-Sepulveda et al.
Unknown**	2	NA	Suri et al. Thacker et al.

*The validated or estimated sequence is neither available through the published manuscripts or the Infevers database as of June 25, 2024. **The precise nucleotide position has not been formally reported in the published manuscript or any other public sources.

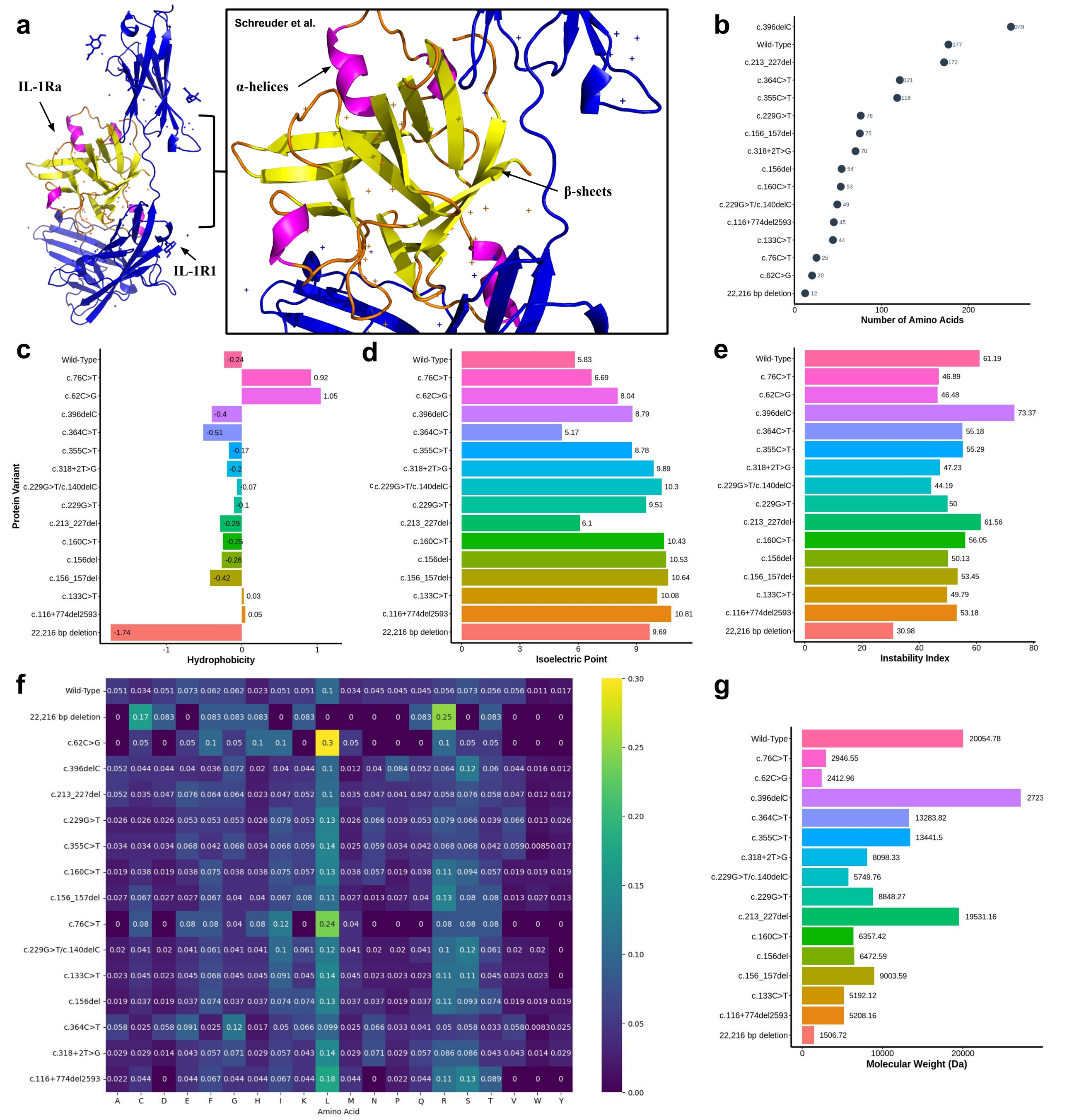
a
IL-1Ra
IL-1R1
Schreuder et al.
α-helices
β-sheets
b
c.396delC 249
Wild-Type 177
c.213_227del 172
c.364C>T 121
c.355C>T 118
c.229G>T 76
c.156_157del 75
c.318+2T>G 70
c.156del 54
c.160C>T 53
c.229G>T/c.140delC 49
c.116+774del2593 45
c.133C>T 44
c.76C>T 25
c.62C>G 20
22,216 bp deletion 12
0 100 200
Number of Amino Acids
c
Protein Variant
Wild-Type -0.24
c.76C>T 0.92
c.62C>G 1.05
c.396delC -0.4
c.364C>T -0.51
c.355C>T -0.17
c.318+2T>G -0.2
c.229G>T/c.140delC -0.07
c.229G>T -0.1
c.213_227del -0.29
c.160C>T -0.25
c.156del -0.26
c.156_157del -0.42
c.133C>T 0.03
c.116+774del2593 0.05
22,216 bp deletion -1.74
-1 0 1
Hydrophobicity
d
Wild-Type 5.83
c.76C>T 6.69
c.62C>G 8.04
c.396delC 8.79
c.364C>T 5.17
c.355C>T 8.78
c.318+2T>G 9.89
c.229G>T/c.140delC 10.3
c.229G>T 9.51
c.213_227del 6.1
c.160C>T 10.43
c.156del 10.53
c.156_157del 10.64
c.133C>T 10.08
c.116+774del2593 10.81
22,216 bp deletion 9.69
0 3 6 9
Isoelectric Point
e
Wild-Type 61.19
c.76C>T 46.89
c.62C>G 46.48
c.396delC 73.37
c.364C>T 55.18
c.355C>T 55.29
c.318+2T>G 47.23
c.229G>T/c.140delC 44.19
c.229G>T 50
c.213_227del 61.56
c.160C>T 56.05
c.156del 50.13
c.156_157del 53.45
c.133C>T 49.79
c.116+774del2593 53.18
22,216 bp deletion 30.98
0 20 40 60 80
Instability Index
f
Wild-Type 0.051 0.034 0.051 0.073 0.062 0.062 0.023 0.051 0.051 0.1 0.034 0.045 0.045 0.045 0.056 0.073 0.056 0.056 0.011 0.017
22,216 bp deletion 0 0.17 0.083 0 0.083 0.083 0.083 0 0.083 0 0 0 0 0.083 0.25 0 0.083 0 0 0
c.62C>G 0 0.05 0 0.05 0.1 0.05 0.1 0.1 0 0.3 0.05 0 0 0 0.1 0.05 0.05 0 0 0
c.396delC 0.052 0.044 0.044 0.04 0.036 0.072 0.02 0.04 0.044 0.1 0.012 0.04 0.084 0.052 0.064 0.12 0.06 0.044 0.016 0.012
c.213_227del 0.052 0.035 0.047 0.076 0.064 0.064 0.023 0.047 0.052 0.1 0.035 0.047 0.041 0.047 0.058 0.076 0.058 0.047 0.012 0.017
c.229G>T 0.026 0.026 0.026 0.053 0.053 0.053 0.026 0.079 0.053 0.13 0.026 0.066 0.039 0.053 0.079 0.066 0.039 0.066 0.013 0.026
c.355C>T 0.034 0.034 0.034 0.068 0.042 0.068 0.034 0.068 0.059 0.14 0.025 0.059 0.034 0.042 0.068 0.068 0.042 0.059 0.0085 0.017
c.160C>T 0.019 0.038 0.019 0.038 0.075 0.038 0.038 0.075 0.057 0.13 0.038 0.057 0.019 0.038 0.11 0.094 0.057 0.019 0.019 0.019
c.156_157del 0.027 0.067 0.027 0.027 0.067 0.04 0.04 0.067 0.08 0.11 0.027 0.013 0.027 0.04 0.13 0.08 0.08 0.013 0.027 0.013
c.76C>T 0 0.08 0 0.08 0.08 0.04 0.08 0.12 0 0.24 0.04 0 0 0 0.08 0.08 0.08 0 0 0
c.229G>T/c.140delC 0.02 0.041 0.02 0.041 0.061 0.041 0.041 0.1 0.061 0.12 0.041 0.02 0.02 0.041 0.1 0.12 0.061 0.02 0.02 0
c.133C>T 0.023 0.045 0.023 0.045 0.068 0.045 0.045 0.091 0.045 0.14 0.045 0.023 0.023 0.023 0.11 0.11 0.045 0.023 0.023 0
c.156del 0.019 0.037 0.019 0.037 0.074 0.037 0.037 0.074 0.074 0.13 0.037 0.037 0.019 0.037 0.11 0.093 0.074 0.019 0.019 0.019
c.364C>T 0.058 0.025 0.058 0.091 0.025 0.12 0.017 0.05 0.066 0.099 0.025 0.066 0.033 0.041 0.05 0.058 0.033 0.058 0.0083 0.025
c.318+2T>G 0.029 0.029 0.014 0.043 0.057 0.071 0.029 0.057 0.043 0.14 0.029 0.071 0.029 0.057 0.086 0.086 0.043 0.043 0.014 0.029
c.116+774del2593 0.022 0.044 0 0.044 0.067 0.044 0.044 0.067 0.044 0.18 0.044 0 0.022 0.044 0.11 0.13 0.089 0 0 0
A C D E F G H I K L M N P Q R S T V W Y
Amino Acid
0.30 0.25 0.20 0.15 0.10 0.05 0.00
g
Wild-Type 20054.78
c.76C>T 2946.55
c.62C>G 2412.96
c.396delC 2723
c.364C>T 13283.82
c.355C>T 13441.5
c.318+2T>G 8098.33
c.229G>T/c.140delC 5749.76
c.229G>T 8848.27
c.213_227del 19531.16
c.160C>T 6357.42
c.156del 6472.59
c.156_157del 9003.59
c.133C>T 5192.12
c.116+774del2593 5208.16
22,216 bp deletion 1506.72
0 10000 20000
Molecular Weight (Da)

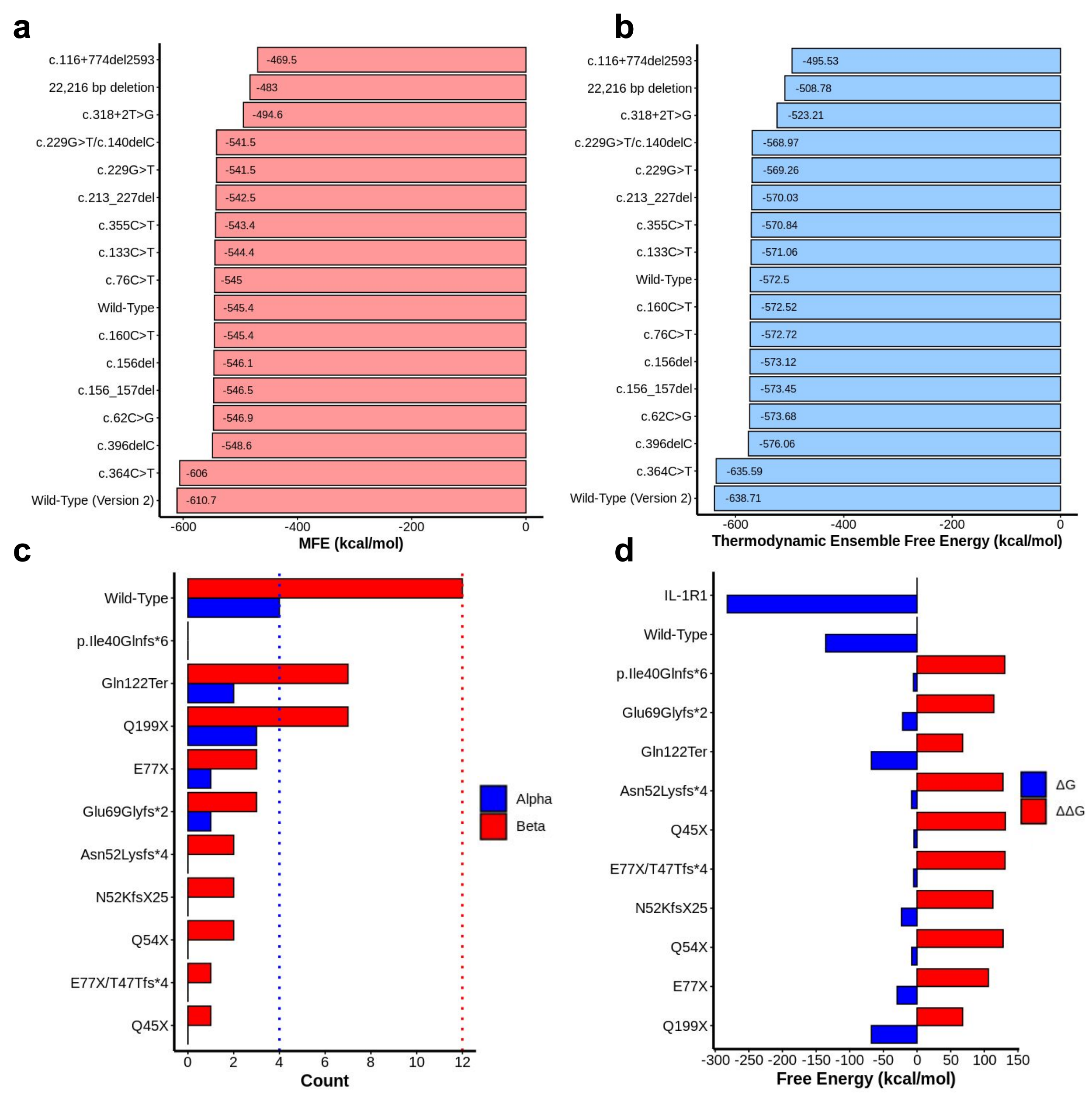
a
c.116+774del2593
22,216 bp deletion
c.318+2T>G
c.229G>T/c.140delC
c.229G>T
c.213_227del
c.355C>T
c.133C>T
c.76C>T
Wild-Type
c.160C>T
c.156del
c.156_157del
c.62C>G
c.396delC
c.364C>T
Wild-Type (Version 2)
-469.5
-483
-494.6
-541.5
-541.5
-542.5
-543.4
-544.4
-545
-545.4
-545.4
-546.1
-546.5
-546.9
-548.6
-606
-610.7
-600
-400
-200
0
MFE (kcal/mol)
b
c.116+774del2593
22,216 bp deletion
c.318+2T>G
c.229G>T/c.140delC
c.229G>T
c.213_227del
c.355C>T
c.133C>T
Wild-Type
c.160C>T
c.76C>T
c.156del
c.156_157del
c.62C>G
c.396delC
c.364C>T
Wild-Type (Version 2)
-495.53
-508.78
-523.21
-568.97
-569.26
-570.03
-570.84
-571.06
-572.5
-572.52
-572.72
-573.12
-573.45
-573.68
-576.06
-635.59
-638.71
-600
-400
-200
0
Thermodynamic Ensemble Free Energy (kcal/mol)
c
Wild-Type
p.Ile40Glnfs*6
Gln122Ter
Q199X
E77X
Glu69Glyfs*2
Asn52Lysfs*4
N52KfsX25
Q54X
E77X/T47Tfs*4
Q45X
0
2
4
6
8
10
12
Count
Alpha
Beta
d
IL-1R1
Wild-Type
p.Ile40Glnfs*6
Glu69Glyfs*2
Gln122Ter
Asn52Lysfs*4
Q45X
E77X/T47Tfs*4
N52KfsX25
Q54X
E77X
Q199X
-300 -250 -200 -150 -100 -50 0 50 100 150
Free Energy (kcal/mol)
ΔG
ΔΔG

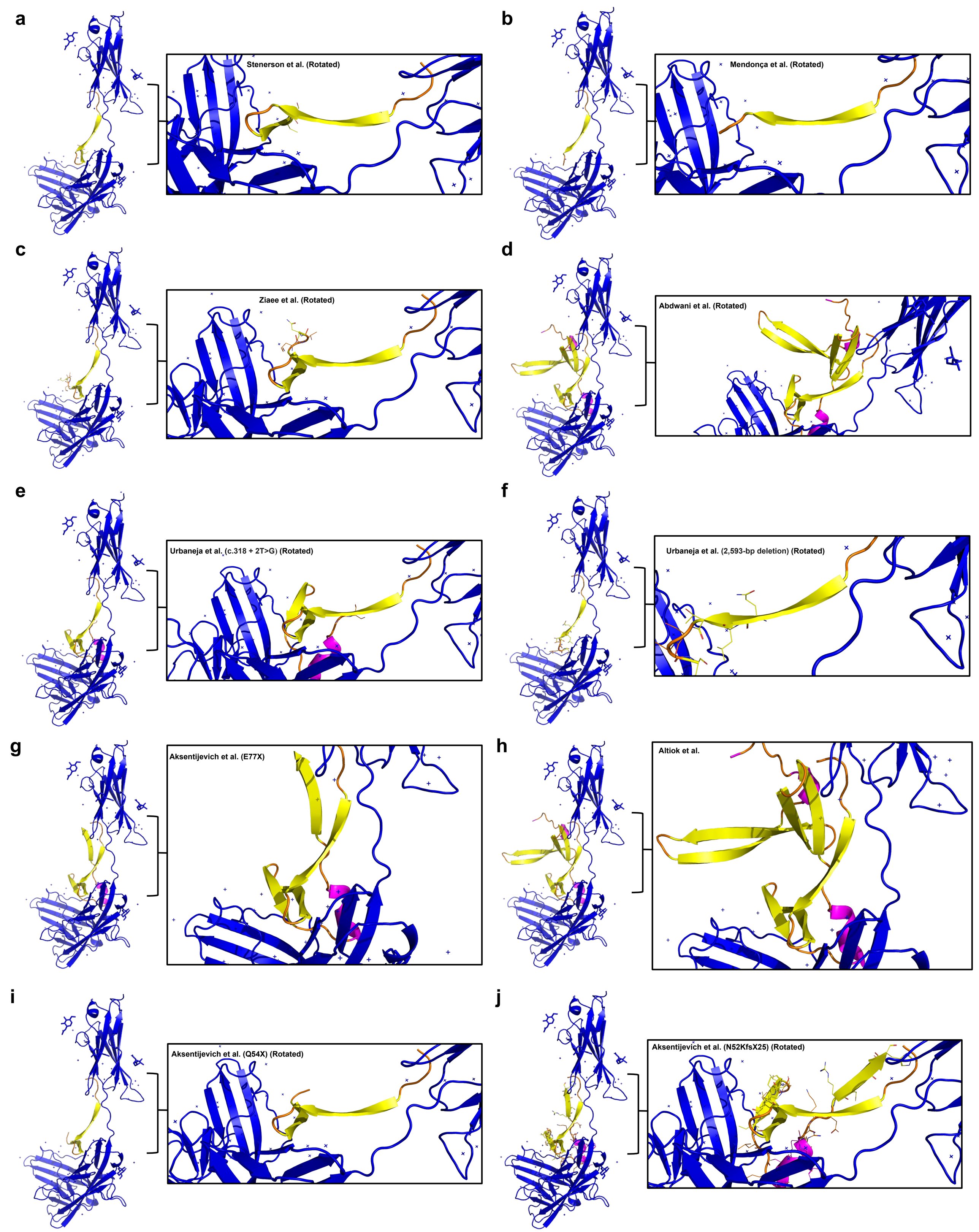
a
Stenerson et al. (Rotated)
b
Mendonça et al. (Rotated)
c
Ziaee et al. (Rotated)
d
Abdwani et al. (Rotated)
e
Urbaneja et al. (c.318 + 2T>G) (Rotated)
f
Urbaneja et al. (2,593-bp deletion) (Rotated)
g
Aksentijevich et al. (E77X)
h
Altiok et al.
i
Aksentijevich et al. (Q54X) (Rotated)
j
Aksentijevich et al. (N52KfsX25) (Rotated)